Atmospheric Environment 284 (2022) 119216

Contents lists available at ScienceDirect

Atmospheric Environment

journal homepage: www.elsevier.com/locate/atmosenv

Impact of COVID-19 restrictions on the dry deposition fraction of settleable particulate matter at three industrial urban/suburban locations in northern Spain

Rosa Lara [a], Laura Megido [a,*], Luis Negral [b], Beatriz Suárez-Peña [c], Leonor Castrillón [a]

[a] Department of Chemical and Environmental Engineering, Polytechnic School of Engineering, Gijón Campus, University of Oviedo, 33203, Gijón, Spain
[b] Department of Chemical and Environmental Engineering, Technical University of Cartagena, Cartagena, Spain
[c] Department of Materials Science and Metallurgical Engineering, Polytechnic School of Engineering, Gijón Campus, University of Oviedo, 33203, Gijón, Spain

HIGHLIGHTS

- High levels of dry deposition were registered at industrialized urban/sub-urban sites.
- Changes in anthropogenic activities lead to changes in settleable particulate matter.
- During lockdown, mean reductions in the levels of dry deposition were 73.5–97.2%.
- Levels of Al, Ca, Fe, Mg, Mn and Na decreased by >75% during lockdown, but not K.
- Wind gusts and certain wind directions were linked to DSPM levels and its components.

GRAPHICAL ABSTRACT

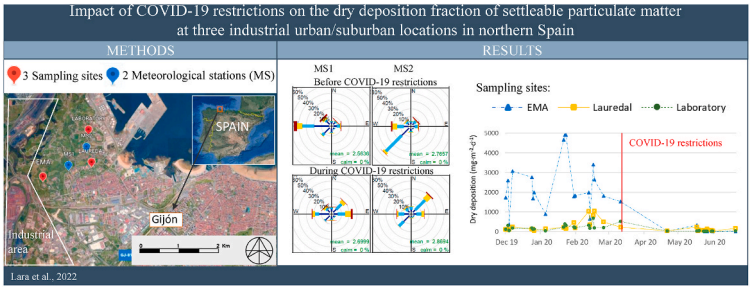

ARTICLE INFO

Keywords:
Air quality
Atmospheric dry deposition
Lockdown
Meteorology
Wind direction

ABSTRACT

Ninety 24-h samples of the dry deposition fraction of settleable particulate matter (DSPM) were collected at one suburban industrial site ('EMA') and two urban industrial sites ('Lauredal' and 'Laboratory') in the western area of Gijón (North of Spain) from December 2019 to June 2020. The levels registered point to an environmental issue that should receive close attention from environmental authorities. Before lockdown restrictions due to COVID-19 were established, all samples collected at the EMA site exceeded 300 $mg{\cdot}m^{-2}{\cdot}d^{-1}$ (the Spanish limit value until 2002). Large amounts of DSPM were also registered at the Lauredal and Laboratory sites, maximum levels reaching 1039.2 and 672.7 $mg{\cdot}m^{-2}{\cdot}d^{-1}$, respectively. Seven metals were analysed in DSPM samples: Al, Ca, Fe, K, Mg, Mn and Na. Fe reached the highest values: 2473.4, 463.4 and 293.3 $mg{\cdot}m^{-2}{\cdot}d^{-1}$ (EMA, Lauredal and Laboratory sites, respectively). This study quantifies the reductions in the DSPM levels registered (on average, 97.2, 73.5 and 90.5% at the EMA, Lauredal and Laboratory sites, respectively) during the lockdown, which involved the restriction of population mobility and industrial activity. The influence of wind speed and its direction were also assessed to better understand the role of these restrictions in the observed reductions. The concentrations of all the metals in the DSPM were reduced by more than 75%, on average, except for K at the Laboratory and Lauredal sites. These decreases were much higher than those found by other authors for smaller fractions of the atmospheric particulate matter (PM10, PM2.5). The findings of the present study highlight the

* Corresponding author.
E-mail address: megidolaura@uniovi.es (L. Megido).

https://doi.org/10.1016/j.atmosenv.2022.119216
Received 2 April 2022; Received in revised form 28 May 2022; Accepted 29 May 2022
Available online 31 May 2022

importance of DSPM in highly industrialized urban/suburban locations and indicate the direction that legal measures might take, given the influence of anthropogenic emissions.

1. Introduction

The first case of COVID-19 was reported in the region of Wuhan in Hubei (China) at the end of 2019 and spread rapidly to other countries around the world. Consequently, the World Health Organization (WHO) declared the COVID-19 pandemic in March 2020 (WHO, 2020). The pandemic has caused enormous challenges in countries around the world in the social, economic, environmental and health fields, among others (Gautam and Hens, 2020; Khalifa et al., 2021). The lockdown decreed by the Spanish Government involved severe restrictions on human activities, including industry and urban mobility (Querol et al., 2021), from March 14, 2020 to June 21, 2020 (MPRCMD, 2020).

Different authors have studied the influence of the pandemic on air quality. A comparative study of the concentration of PM2.5 in the 50 most polluted capital cities in the world was carried out by Rodríguez-Urrego and Rodríguez-Urrego (2020). This study compared pollution during a typical time of normal mobility and during the lockdown and found a reduction of 12% on average for PM2.5. Briz-Redón et al. (2022, 2021) investigated the impact of a short-term lockdown during the period from March 15, 2020 to April 12, 2020 on atmospheric pollutants in several representative Spanish cities, finding reductions in the levels of NO_2, CO, SO_2 and PM10. However, they found an increasing trend of PM2.5 levels in the minor lockdown (from March 15, 2020 to March 29, 2020) and O_3 levels in the whole period. Tobías et al. (2020) studied the influence of the pandemic on PM10, NO_2, SO_2, O_3 and black carbon (BC). After two weeks of lockdown, urban air pollution decreased, but with substantial differences among the pollutants. The most significant reduction was measured for BC and NO_2 (45–51%). A lower reduction was observed for PM10 (28–31%). By contrast, O_3 levels increased (33–57%). In the United Kingdom, Jephcote et al. (2021) analysed daily pollutant measurements of NO_2, O_3 and PM2.5 during the period from March 30, 2020 to May 05, 2020 across the United Kingdom and contrasted them with measurements over the same period during 2017–2019. These authors identified mean reductions in NO_2 of 38.3% and in PM2.5 of 16%, while O_3 concentrations increased by 8%, on average. Shehzad et al. (2020) studied the influence of the pandemic on the concentration of NO_2 in Mumbai and Delhi, two of the most heavily populated cities in India. A substantial decrease in NO_2 (40–50%) was observed in comparison with the same period of the previous year. Kumari and Toshniwal (2020) analysed the differences between the monthly concentrations of air pollutants in March, April, and May of 2020 with those of the same months of 2019 in 12 major cities across the globe. The concentration of PM2.5, PM10 and NO_2 were reduced by 20–34%, 24–47% and 32–64%, respectively. However, a lower reduction in SO_2 was observed and O_3 levels increased. In an urban area of Graz, Austria, Lovrić et al. (2021) analysed the influence of lockdown on the concentration of NO_2, PM10 and O_3, finding that the reductions in the average concentration for the lockdown period were: 37–42%, and 7–14% for NO_2 and PM10, respectively. As in the previous studies, an increase of 12–34% for O_3 was measured.

To sum up, recent studies revealed the effect produced by the lockdown in urban areas on the basis of mainly four pollutants: a decrease in the concentration of NO_2 and to a lesser extent, a decrease in PM10 and PM2.5 in the atmosphere and a relative increase in O_3 concentration. This increase might be explained by three factors: the NO_x reduction in a VOCs-limited environment, NO reduction leading to a reduction in O_3 and higher insolation and temperatures (Tobías et al., 2020).

To the best of our knowledge, the influence of lockdown on settleable particulate matter (SPM) has not been analysed yet, perhaps because there is currently no legislation for this pollutant in many countries of the world. For example, in Spain the limit value was 300 $mg \cdot m^{-2}$ (mean concentration in 24 h) until 2002, when its regulation was repealed (by Royal Decree 1073/2002).

However, the negative effects of SPM both on vegetation and on materials and buildings (modification of their properties, discoloration, degradation, etc.), and the complaints of the population living in areas with SPM levels of <333 $mg \cdot m^{-2} \cdot d^{-1}$ were highlighted by other authors (Mohapatra and Biswal, 2014; Machado et al., 2018).

This study aims to assess whether there was a significant reduction in the dry deposition fraction of the SPM (DSPM) during the restriction of population mobility and industrial activity caused by COVID-19 in two urban sites and one suburban site in an industrialized city in the north of Spain (Gijón). Seven metals in DSPM were also assessed. Furthermore, the speed and direction of wind was analysed in order to evaluate the influence of these meteorological variables on the observed reductions.

2. Materials and methods

2.1. Studied area

The present study was carried out simultaneously at three sampling sites in an industrialized area in the western boroughs of Gijon, a city on the northern coast of Spain. Fig. 1 shows the location of these three sampling sites ("EMA", "Lauredal" and "Laboratory") and the two meteorological stations ("MS1" and "MS2") used for this study, together with the main industrial activities in their surroundings.

"EMA" (43°32′24.2″N 5°43′01.3″W, 60 m AMSL) is a suburban site, whereas "Lauredal" (43°32′35.47″N 5°42′9.50″W, 33 m AMSL) and "Laboratory" (43°33′0.72″N 5°42′12.77″W, 20 m AMSL) are urban sites.

According to the public information provided by the Spanish Register of Emissions and Pollutant Sources (PRTR, 2020), the industries with the highest emissions of PM10 during 2019 (3 km around the sampling site) were: a steelworks (544 $t \cdot y^{-1}$, including also the PM10 emissions of a factory located 10 km away), a coal-fired power plant (92.7 $t \cdot y^{-1}$) and a cement factory (36.4 $t \cdot y^{-1}$) (Fig. 1). Furthermore, there is a stockyard and a Port of $4.15 \cdot 10^6$ m^2 with a movement of bulk commodities (mainly coal, iron ore and cement) of 862979 $t \cdot y^{-1}$ in 2019 (APG, 2020) which, being handled and stored in the open air, may lead to significant diffuse emissions of particles by the action of the wind.

2.2. Sampling

90 samples of DSPM were collected, 30 at each sampling site simultaneously. The collectors used were described by Negral et al. (2021): a 1-m^2 tray with detachable side walls of 0.05 m in height that avoid the loss of dry matter after being deposited. All the equipment parts were made of methacrylate in order to avoid any reaction between the samples and the surface collector. Methacrylate is a suitable material because the carbonaceous fraction was not studied.

Each DSPM sample was collected during 24 h from 4 p.m. on one day to 4 p.m. on the following day. The samples were named according to this latter date. In the case of rain being detected, the sample was discarded. Thus, sampling dates were intermittent.

The sampling was carried out from December 4, 2019 to June 23, 2020. In order to assess the impact that the lockdown restrictions from mid-March 2020 had on DSPM concentrations, the study was divided into two periods of time: before restrictions (from March 12, 2019 to March 14, 2020, $n = 19$ samples per site) and during restrictions (from March 15, 2020 to June 23, 2020, $n = 11$ samples per site). It should be noticed that samples collected on June 23, 2020 have been included in the second group as this date was very close in time to the other sampling days, even though the official lockdown had finished two days

before.

2.3. Metals

The DSPM collected was gravimetrically determined and chemically digested by HF, HNO_3 and $HClO_4$ for metal extraction, as in a previous study (Negral et al., 2021). Subsequently, seven metals (Al, Ca, Fe, K, Mg, Mn and Na) were analysed in the 90 DSPM samples by inductively coupled plasma mass spectrometry (ICP-MS) using an Agilent 7700X system. The procedure was applied in parallel to a sample of Standard Reference Material® 1648a for urban particulate matter from the National Institute of Standards and Technology (NIST) and a blank sample in order to ensure the analytical quality of results. Errors remained below 10%.

2.4. Meteorological data

Meteorological data were registered throughout the studied period by means of two meteorological stations (Fig. 1): "MS1" (43°32′33.2″N 5°42′34.0″W, 20 m AMSL) and "MS2" (43°32′47.9″N 5°42′14.5″W, 125 m AMSL), which belong to the City Council of Gijón and the Regional Government of the Principality of Asturias, respectively. Considering their location with respect to the sampling sites and the topographic characteristics of the area, the meteorological dataset from MS1 was assigned to the EMA and Lauredal sites and that from MS2 to the Laboratory site.

The recorded values were hourly averages, resulting in a total of 24 values per day. 24-h wind roses were created covering the same periods of time as the DSPM sampling periods by means of the openair package in the R4.0.4 software (Carslaw and Ropkins, 2012). Eight wind directions were considered, each of them being represented by a circular sector whose limit corresponded to the value of the central angle ±22.5°.

The maximum daily wind speed and the wind direction to which it was associated for each DSPM sample were identified in order to analyse whether there was a relationship between the maximum wind gusts and the amount of dry matter collected.

2.5. Statistics

Statistical studies were carried out using R4.0.4 software. A p-value < 0.05 was considered statistically significant.

The distribution of the collected data was analysed by the Shapiro-Wilk normality test, resulting in the conclusion that none of the variables studied presented a normal distribution. The Kruskal–Wallis test was used to determine if there were significant differences between sampling sites in the mean levels of particles and metallic elements in DSPM. As significant differences were found, the following tests were done independently for each sampling site. The Kruskal-Wallis test was also used to assess significant differences depending on the mean wind direction of each sample collected. Due to the small sample size, four directions were considered (N, E, S and W, each of them being represented by a circular sector whose limit corresponded to the value of the central angle ±45°). The Mann–Whitney U test was used to determine if there were significant differences between the means of the samples collected before and after restrictions. Boxplots of the levels of particles and metallic elements in DSPM were provided in Supplementary Material (Figs. S1–S8). Furthermore, correlations between DSPM levels of the components measured in the DSPM samples and with the maximum wind speed were studied by Spearman correlation coefficients (r_s). These tests have been used by other authors to evaluate changes in air pollution during restrictions (Silva et al., 2022).

3. Results and discussion

3.1. DSPM levels

DSPM levels showed great variability regardless of the period of time considered during the sampling campaign (before or during restrictions), ranging from 5.0 to 4901.0 $mg{\cdot}m^{-2}{\cdot}d^{-1}$ at the EMA site, 35.0–1039.2 $mg{\cdot}m^{-2}{\cdot}d^{-1}$ at the Lauredal site and 10.4–672.7 $mg{\cdot}m^{-2}{\cdot}d^{-1}$ at the Laboratory site (Table 1). The mean values were 1529.1 $mg{\cdot}m^{-2}{\cdot}d^{-1}$, 234.8 $mg{\cdot}m^{-2}{\cdot}d^{-1}$ and 158.0 $mg{\cdot}m^{-2}{\cdot}d^{-1}$, respectively.

A previous study of DSPM levels was carried out at the Lauredal and Laboratory sites from March to June 2019 (Negral et al., 2021), in which

Fig. 1. Studied area: sampling sites and industrial activities (image created using Google Earth and AutoCAD, 2015).

Table 1
Minimum, mean and maximum DSPM levels in $mg{\cdot}m^{-2}{\cdot}d^{-1}$ at the three sampling sites for the whole sampling period and before and after the COVID-19 restrictions were established.

Sampling station	Before restrictions (n = 19)					During restrictions (n = 11)					Total (n = 30)		
	Min.	Mean ± SD			Max.	Min.	Mean ± SD			Max.	Mean ± SD		
EMA (n = 30)	359.0	2375.3	±	1331.8	4901.0	5.0	67.6	±	95.6	330.3	1529.1	±	1543.7
Lauredal (n = 30)	45.2	321.5	±	311.9	1039.2	35.0	85.1	±	61.9	229.7	234.8	±	274.1
Laboratory (n = 30)	36.2	236.6	±	156.3	672.7	10.4	22.4	±	9.8	42.1	158.0	±	161.9

the samples collected varied between 34.3 and 830.3 $mg{\cdot}m^{-2}{\cdot}d^{-1}$ and 8.6–307.2 $mg{\cdot}m^{-2}{\cdot}d^{-1}$, respectively. These values were higher than those recorded at the same sites during the same period in 2020 (35–229.7 $mg{\cdot}m^{-2}{\cdot}d^{-1}$ at the Lauredal site and 10.4–42.1 $mg{\cdot}m^{-2}{\cdot}d^{-1}$ at the Laboratory site); which may be explained by the lower anthropogenic activity due to the lockdown restrictions. In fact, the order of magnitude of the samples collected in that study of 2019 was more in agreement with the levels obtained before the restrictions (45.2–1039.2 $mg{\cdot}m^{-2}{\cdot}d^{-1}$ and 36.2–672.7 $mg{\cdot}m^{-2}{\cdot}d^{-1}$).

In general, the highest levels of DSPM were registered at the EMA site, which is closer to the facilities of a steelworks than the other two sampling sites (Fig. 1). Significant differences ($p < 0.05$) were

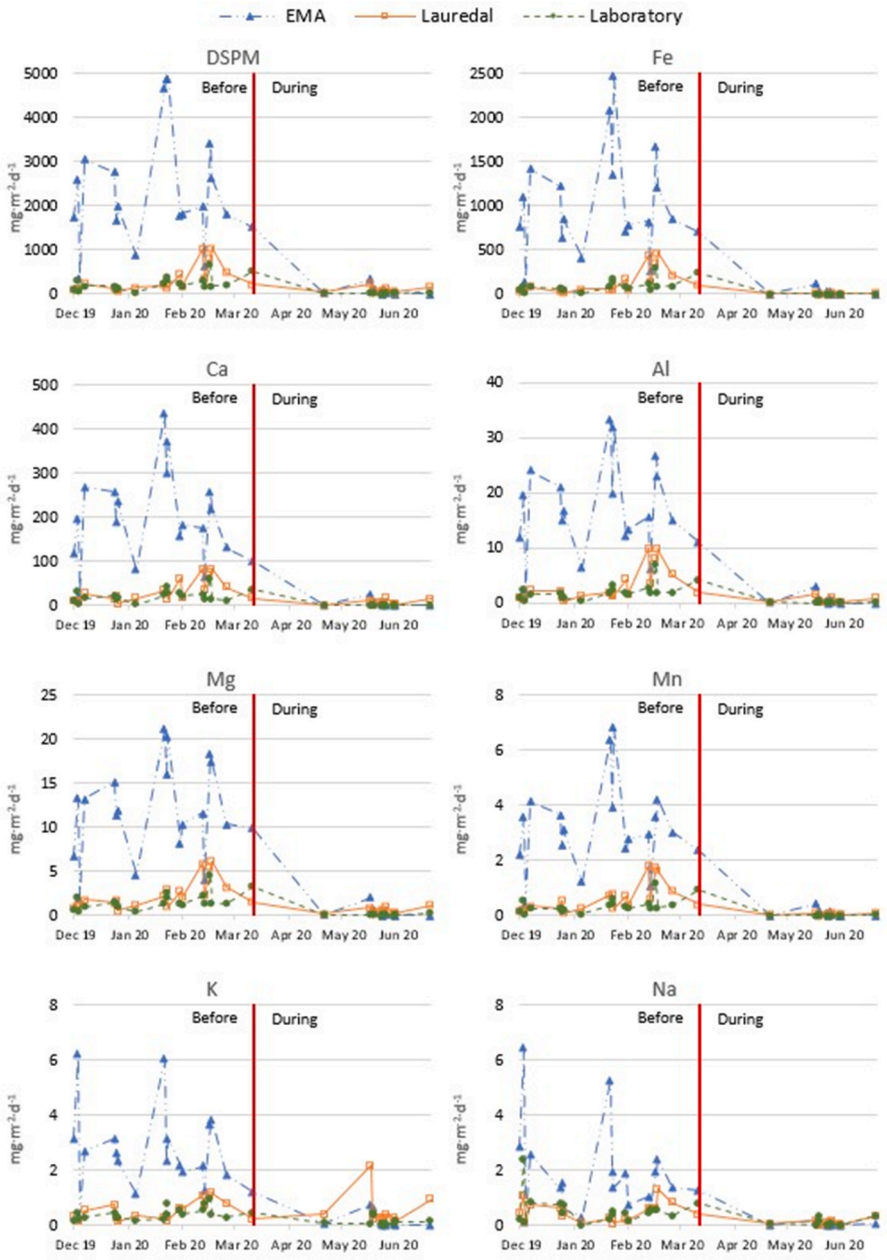

Fig. 2. DSPM, Fe, Ca, Al, Mg, Mn, K and Na levels of 24-h samples from December 2019 to June 2020 at three industrial suburban/urban sites ('EMA', 'Lauredal' and 'Laboratory'). Red vertical line indicates the beginning of the restrictions due to COVID-19. (For interpretation of the references to color in this figure legend, the reader is referred to the Web version of this article.)

determined between the EMA site and the others, being mean value one order of magnitude higher than at the other two sampling locations, considering both the whole sampling campaign and the period of time before restrictions (Table 1). However, this marked difference in the DSPM levels between the three sampling locations was not observed after mid-March 2020. Once the strict lockdown measurements were enforced and there was an abrupt reduction of human and industrial activities, DSPM levels underwent a significant reduction ($p < 0.05$), which was more evident at the EMA site precisely due to the higher values recorded overall at that location. Fig. 2 shows the temporal variation in DSPM levels at the three sampling sites, the major reduction during restrictions being evident.

During the lockdown, although the maximum DSPM value was recorded at the EMA site (330.3 $mg{\cdot}m^{-2}{\cdot}d^{-1}$), it was the Lauredal site which had the highest mean DSPM levels (20.6 and 73.7% higher than those registered at the EMA and Laboratory stations, respectively). Nonetheless, these differences in the mean values should be considered with caution, given the variability observed in the dataset.

Significant reductions ($p < 0.05$) were registered during the restrictions in the mean DSPM levels: 97.2 ± 78.3%, 73.5 ± 122.0% and 90.5 ± 89.2% at the EMA, Lauredal and Laboratory sites, respectively. These reductions were higher than those found by other authors for other fractions of atmospheric particulate matter, as stated in the Introduction section (i.e., 7–47% for PM10 and 12–34% for PM2.5).

The great variability in the dataset lead to high standard deviations for these calculated reductions. Tobías et al. (2020) and Ravindra et al. (2022) highlighted the role of meteorology in the variability of their dataset. They stated that lower reductions may be attributed to unfavourable meteorology and pointed out the caution with which changes in atmospheric pollutant levels should be evaluated because of the number of factors involved. Briz-Redón et al. (2022, 2021) fitted pollutant levels through a statistical model considering meteorological variables (temperature, wind speed, sunlight hours and max pressure), weekend days and lockdown periods of time.

3.2. Metals

Seven metals were analysed in the DSPM fraction at the three sampling sites. Comparing the levels of these elements between the three sampling sites (Figs. S1–S18), significant differences ($p < 0.05$) were found between those determined at the EMA site and the other two sites, except in the case of Ca and Na. Ca data only presented significant differences between the EMA and the Laboratory sites. Na did not presented differences between any combination of sampling sites, which is not surprising due to the proximity to the coast. However, significant differences were not found between levels registered at Lauredal and the Laboratory site, regardless of the element considered.

Table 2 shows the minimum, maximum and mean values obtained for the seven elements in DSPM. Among them, Fe was the most abundant element, regardless of the sampling site, with values up to 3.5 times the level of the second most abundant element: Ca.

At the EMA site, Fe concentration reached up to 40% of DSPM in 53% of the samples collected. 87% of these samples were collected before restrictions. The maximum concentration of Fe was recorded on January 26, 2020 (2473.4 $mg{\cdot}m^{-2}{\cdot}d^{-1}$), representing 50.5% of the DSPM sample (Lara et al., 2021). Fe was also the major element recorded at the Lauredal (81.2 $mg{\cdot}m^{-2}{\cdot}d^{-1}$) and the Laboratory (60.5 $mg{\cdot}m^{-2}{\cdot}d^{-1}$) sites, contributing more than 40% to DSPM collected in 16% and 23% of samples respectively. All the samples with such high amount of iron were collected before restrictions. Ca reached mean values of 127.7 $mg{\cdot}m^{-2}{\cdot}d^{-1}$, 23.1 $mg{\cdot}m^{-2}{\cdot}d^{-1}$ and 14.9 $mg{\cdot}m^{-2}{\cdot}d^{-1}$ at the EMA, Lauredal and Laboratory sites, respectively.

Although the seven elements analysed in DSPM are generally associated with crustal sources (Martins et al., 2016; Banerjee et al., 2015; Salvador et al., 2004; Querol et al., 2002; Herut et al., 2001), anthropogenic activities can also contribute. Among these possible sources would be the resuspension of soil dust due to the movement of vehicles in the area and industrial activities, given the proximity of the steelworks, the coal stockyard or the Port to the measurement stations in this study (Fig. 1). Indeed, Fe and Mn are commonly associated with all the processing units of an integrated iron and steel facility (Tsai et al., 2007; Dall'Osto et al., 2008). Hleis et al. (2013) characterized the chemical profile of particle sources at an integrated iron and steel plant in France. They identified Fe, Ca, Al, Mg, Mn and K as important fugitive emissions from a sinter plant. Tsai et al. (2007) identified Na, along with Fe and S, as one of the major elements in particle emission from an integrated iron and steel plant. Nevertheless, these elements may also be provided from other sources. For example, Na is also a tracer for sea salt (Almeida et al., 2005) and K has been widely related to biomass combustion (Alastuey et al., 2016; Banerjee et al., 2015; Nava et al., 2015; Watson et al., 2002), but also to marine aerosol, crustal sources, coal fire or industry (Pachon et al., 2013). At the EMA station, except for K and Na, strong correlations ($r_s > 0.95$) were found between all the metals measured in the DSPM samples collected, which in some cases reached 0.99 (DSPM with Fe and Al with Fe, Mg and Mn). However, at the Lauredal station, such high correlations were only found between Ca–Mg (0.98), Ca–Mn (0.96) and Mg–Mn (0.98). Finally, at the Laboratory site DSPM levels presented good correlations with Ca, Al, Mg and Mn (0.96, 0.97, 0.97 and 0.98, respectively). There was also found significant interdependence of Mn with Fe (0.97), Ca (0.97), Al (0.98) and Mg (0.98) and Mg with Ca and Al (0.96 in both cases).

Table 3 shows the minimum, maximum and mean values obtained for each metal measured in the DSPM samples, distinguishing between the time periods before and during the lockdown restrictions. During the restrictions, significant reductions ($p < 0.05$) were observed for all the metals, except for K at the Lauredal site, whose mean level before and during restrictions were 0.5 ± 0.3 and 0.5 ± 0.6 $mg{\cdot}m^{-2}{\cdot}d^{-1}$, respectively.

Fe was the major component in DSPM samples collected during both periods of time, regardless of the sampling site (Fig. 2), and showed the greatest reduction (Table S1): 97.9, 95.0 and 97.4% at the EMA, Lauredal and Laboratory sites, respectively.

At the EMA site, the reductions observed for each chemical species between the two periods of time were greater than 95%, except for K

Table 2
Minimum, mean, standard deviation and maximum levels of metals in DSPM samples, expressed in $mg{\cdot}m^{-2}{\cdot}d^{-1}$, at the three sampling sites ('EMA, 'Lauredal' and 'Laboratory') during the whole sampling period.

Element	EMA (n = 30)					Lauredal (n = 30)					Laboratory (n = 30)				
	Min.	Mean ± SD			Max.	Min.	Mean ± SD			Max.	Min.	Mean ± SD			Max.
Fe	0.42	656.8	±	678.6	2473.4	1.58	81.2	±	126.3	463.4	1.30	60.5	±	72.9	293.3
Ca	0.35	127.7	±	125.7	437.4	1.30	23.1	±	23.7	84.6	0.39	14.9	±	15.6	62.5
Al	0.03	11.1	±	10.5	33.4	0.21	2.2	±	2.7	10.0	0.09	1.5	±	1.5	6.9
Mg	0.03	7.7	±	7.1	21.1	0.17	1.7	±	1.6	6.1	0.06	1.1	±	1.1	4.5
Mn	0.00	2.1	±	2.0	6.9	0.02	0.4	±	0.5	1.8	0.01	0.2	±	0.3	1.1
K	0.01	1.8	±	1.7	6.2	0.14	0.5	±	0.4	2.2	0.05	0.3	±	0.2	1.0
Na	0.01	1.2	±	1.5	6.5	0.03	0.4	±	0.3	1.3	0.02	0.4	±	0.5	2.4

Table 3
Minimum, mean, standard deviation and maximum metal levels, in $mg \cdot m^{-2} \cdot d^{-1}$, measured in DSPM samples collected at the three sampling sites before and during restrictions.

		Before (n = 19)			During (n = 11)		
Element	Site	Min.	Mean ± SD	Max.	Min.	Mean ± SD	Max.
Fe (n = 30)	EMA	147.87	1024.9 ± 592.8	2473.4	0.42	21.0 ± 32.2	111.8
	Lauredal	11.43	124.7 ± 142.3	463.4	1.58	6.2 ± 5.5	20.3
	Laboratory	12.86	94.1 ± 72.8	293.3	1.30	2.5 ± 1.0	4.8
Ca (n = 30)	EMA	23.26	198.7 ± 104.4	437.4	0.35	5.0 ± 7.3	25.2
	Lauredal	5.65	32.2 ± 25.6	84.6	1.30	7.5 ± 5.1	16.7
	Laboratory	3.20	22.9 ± 14.2	62.5	0.39	1.1 ± 0.7	2.9
Al (n = 30)	EMA	2.37	17.2 ± 8.4	33.4	0.03	0.6 ± 0.9	3.1
	Lauredal	0.41	3.2 ± 3.0	10.0	0.21	0.6 ± 0.5	1.6
	Laboratory	0.33	2.2 ± 1.5	6.9	0.09	0.2 ± 0.1	0.3
Mg (n = 30)	EMA	1.86	11.9 ± 5.4	21.1	0.03	0.4 ± 0.6	2.1
	Lauredal	0.52	2.4 ± 1.7	6.1	0.17	0.6 ± 0.3	1.2
	Laboratory	0.38	1.7 ± 1.0	4.5	0.06	0.1 ± 0.1	0.3
Mn (n = 30)	EMA	0.40	3.2 ± 1.6	6.9	<0.01	0.09 ± 0.1	0.4
	Lauredal	0.08	0.6 ± 0.5	1.8	0.02	0.05 ± 0.02	0.1
	Laboratory	0.05	0.4 ± 0.3	1.2	0.01	0.02 ± 0.01	0.03
K (n = 30)	EMA	0.36	2.7 ± 1.5	6.2	0.01	0.2 ± 0.3	0.8
	Lauredal	0.14	0.5 ± 0.3	1.2	0.15	0.5 ± 0.6	2.2
	Laboratory	0.15	0.4 ± 0.2	1.0	0.05	0.1 ± 0.1	0.5
Na (n = 30)	EMA	0.12	1.9 ± 1.6	6.5	0.01	0.06 ± 0.05	0.2
	Lauredal	0.08	0.5 ± 0.3	1.3	0.03	0.1 ± 0.1	0.4
	Laboratory	0.04	0.6 ± 0.5	2.4	0.02	0.1 ± 0.1	0.4

(92.3%). At the Laboratory site, the reductions were slightly lower than at the EMA site, although all were above 90%, with the exception of K and Na (65.6 and 80.9% respectively). Differing from the other locations, reductions registered at the Lauredal site were considerably lower, but they remained above 70%, except for K, which showed an average increase of 1.6% (Table S1 and Figs. S1–S8).

Nevertheless, it should be born in mind that DSPM levels showed great variability throughout the sampling period, which may have been mainly related to the changes in anthropogenic activities during restrictions, but also to the influence of meteorological conditions, as discussed in section 3.3. The calculated reductions in the DSPM levels and the metals analysed within also reflect such variability.

3.3. Influence of wind speed and wind direction on DSPM levels

DSPM levels are conditioned by multiple factors, such as the proximity and activity of emission sources, which have an influence on their particle size and on their concentration in the atmosphere at a given time. Atmospheric conditions also play an important role in DSPM, modifying the reactivity of pollutants, as well as their displacement speed and deposition velocity. The latter depends on particle size, density and wind speed. For instance, Figgis et al. (2018) demonstrated in a field study that deposition rate increased linearly with wind speed except for episodes with low speed (<3 $m \cdot s^{-1}$), when it seemed to be independent.

Wind roses obtained with the data registered at the MS1 and MS2 are shown in Fig. 3. On average, wind speed was slightly higher at the MS2 station (2.8 ± 1.4 $m \cdot s^{-1}$) than at the MS1 (2.6 ± 1.8 $m \cdot s^{-1}$) throughout the sampling period. As stated in section 2.5, four sectors were considered to evaluate the differences between DSPM levels depending on the mean wind direction of each sample collected (Table 4). The highest DSPM levels were collected on days with W winds, whereas minimum values were associated with N or E winds, depending on the sampling site. None of the samples were associated with S wind.

Meteorological differences between the two sampling periods considered in this study were noticeable, especially regarding the prevailing wind direction. Before restrictions, the dominant wind direction was W at MS1 and SW–W at MS2. Less than 20% of the wind during this period came from the first and second quadrants (N-E and E-S), regardless of the meteorological station. During the restrictions, the wind direction presented more variability, the prevailing wind direction being E at MS1 and NE at MS2. Moreover, mean wind speed was slightly

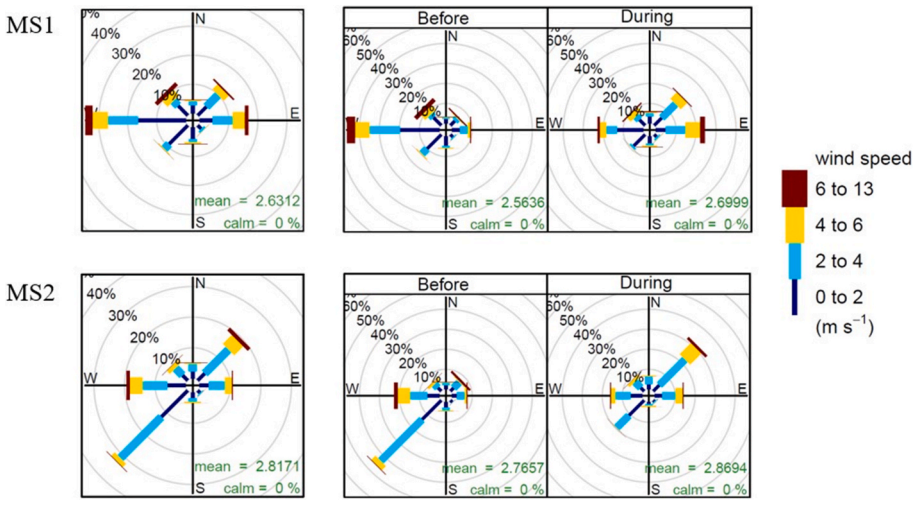

Fig. 3. Wind roses at the meteorological stations MS1 and MS2 considering the whole sampling period (left) and before and during restrictions (right). Concentric circles represent the frequency of counts by wind direction in %. Colours and width paddles indicate wind speed. 'Mean' indicates the mean wind speed and 'calm' is the percentage of cases when wind speed was zero. (For interpretation of the references to color in this figure legend, the reader is referred to the Web version of this article.)

Table 4
Mean DSPM levels, in $mg{\cdot}m^{-2}{\cdot}d^{-1}$, recorded at the three sampling sites (EMA, Lauredal and Laboratory) and distributed with respect to the mean wind of each sample collected, which was recorded at MS1 and MS2.

Wind direction	MS1	EMA		Lauredal		MS2	Laboratory	
	% of days	Mean	SD	Mean	SD	% of days	Mean	SD
N	10	139.8	169.6	100.5	111.9	16.7	120.4	220.1
E	30	205.6	496.7	95.1	61.2	23	22.7	11.4
S	–	–	–	–	–	–	–	–
W	60	2422.5	1353.7	327.1	320	60	221.2	145.3

higher during restrictions at both stations: 2.6 ± 1.9 $m{\cdot}s^{-1}$ before restrictions versus 2.7 ± 1.7 $m{\cdot}s^{-1}$ during restrictions at the MS1 and 2.8 ± 1.4 $m{\cdot}s^{-1}$ before restrictions versus 2.9 ± 1.3 $m{\cdot}s^{-1}$ during restrictions at the MS2.

Significant differences ($p < 0.05$) between the levels in DSPM (for both particles and metallic elements) grouped by the mean wind direction of each sample collected were tested by the Kruskal-Wallis test. At the EMA site, significant differences were found between the levels collected under W and N winds, and also between W and E winds, for all the elements measured. However, at the Laboratory significant differences were only observed under W and E winds for all the elements analysed. At the Lauredal site, significant differences were found between the levels of DSPM and Al collected on days under W and E winds, whereas for Ca, Fe, Mg, Mn and Na differences were also presented between days under W and N winds. On contrast, K presented a different pattern than the rest of the elements measured and no significant differences were found attending to the mean wind direction. The highest levels of K were found to be linked to days under N winds.

3.3.1. Before restrictions

Before restrictions, all DSPM samples collected at the EMA site exceeded 300 $mg{\cdot}m^{-2}{\cdot}d^{-1}$, reaching levels up to 4000 $mg{\cdot}m^{-2}{\cdot}d^{-1}$ in three of the samples collected in January: on January 24, 2020 (4659.5 $mg{\cdot}m^{-2}{\cdot}d^{-1}$), on January 25, 2020 (4901.0 $mg{\cdot}m^{-2}{\cdot}d^{-1}$) and on January 26, 2020 (4898.4 $mg{\cdot}m^{-2}{\cdot}d^{-1}$). On these days, the prevailing wind direction was from W-SW (> 65% frequency of counts of wind direction during these sampling days) and the mean wind speed was 1.3 ± 0.3 $m{\cdot}s^{-1}$. There were three days on which DSPM levels fell below 1000 $mg{\cdot}m^{-2}{\cdot}d^{-1}$ at the EMA site. During two of them (December 7, 2019 with 359.0 $mg{\cdot}m^{-2}{\cdot}d^{-1}$ and January 8, 2020 with 887.2 $mg{\cdot}m^{-2}{\cdot}d^{-1}$), the prevailing winds were W and the wind speeds were 3.0 ± 1.1 $m{\cdot}s^{-1}$ and 2.5 ± 0.9 $m{\cdot}s^{-1}$ respectively. Due to a higher speed, the particles may have remained longer in the atmosphere and have been carried further away, thus decreasing the DSPM levels. On the contrary, the third day (February 16, 2020 with 649.1 $mg{\cdot}m^{-2}{\cdot}d^{-1}$) was characterized by a very low wind speed (0.8 ± 0.1 $m{\cdot}s^{-1}$) and prevailing wind from W-SW (> 49% frequency of counts). Wind roses corresponding to samples with maximum and minimum DSPM levels before and during restrictions can be consulted in the Supplementary Material (Figs. S9 and S10). Those corresponding to the Lauredal and Laboratory site are also included (Figs. S11–S14) and are described below.

At the Lauredal site, only 31% of the samples collected before restrictions exceeded 300 $mg{\cdot}m^{-2}{\cdot}d^{-1}$. DSPM levels greater than 1000 $mg{\cdot}m^{-2}{\cdot}d^{-1}$ were collected on two occasions: on February 15, 2020 (1029.2 $mg{\cdot}m^{-2}{\cdot}d^{-1}$) and on February 20, 2020 (1039.2 $mg{\cdot}m^{-2}{\cdot}d^{-1}$). Wind roses for these two sampling days indicate a higher frequency of W winds (more than 35% frequency of counts by wind direction on both days), with wind speeds of 1.3 ± 0.8 $m{\cdot}s^{-1}$ and 1.6 ± 0.9 $m{\cdot}s^{-1}$, respectively. Minimum DSPM values were registered on days with different wind profiles. For example, on December 6, 2019, 88.5 $mg{\cdot}m^{-2}{\cdot}d^{-1}$ were collected, with a prevailing wind from the SW and wind speed of 2.2 ± 0.9 $m{\cdot}s^{-1}$; whereas on December 29, 2019, 45.2 $mg{\cdot}m^{-2}{\cdot}d^{-1}$ were measured, with gentle winds (1.2 ± 0.4 $m{\cdot}s^{-1}$) mainly from the W.

At the Laboratory site, 26% of the samples taken before restrictions exceeded 300 $mg{\cdot}m^{-2}{\cdot}d^{-1}$, with maximums of 672.7 $mg{\cdot}m^{-2}{\cdot}d^{-1}$ on February 19, 2020 (75% of wind from W with 2.1 ± 1.1 $m{\cdot}s^{-1}$ wind speed on average) and 513.9 $mg{\cdot}m^{-2}{\cdot}d^{-1}$ on March 14, 2020 (great variability in wind direction with predominant winds from NE and SW and 1.99 $m{\cdot}s^{-1}$ on average). Wind roses associated with the lowest DSPM levels (December 7, 2019 and January 8, 2020, with 49.5 and 36.2 $mg{\cdot}m^{-2}{\cdot}d^{-1}$, respectively) presented predominant SW winds with a frequency greater than 79% and mean wind speeds of 2.7 ± 0.7 $m{\cdot}s^{-1}$ and 2.9 ± 0.9 $m{\cdot}s^{-1}$, respectively.

3.3.2. During restrictions

During restrictions, the maximum DSPM level reached at the EMA site was 330.3 $mg{\cdot}m^{-2}{\cdot}d^{-1}$ on May 20, 2020 when the mean wind speed was 3.1 ± 1.7 $m{\cdot}s^{-1}$. Prevailing winds that day came from the W and NE. Minimum levels of DSPM were registered on May 27, 2020 with 5.5 $mg{\cdot}m^{-2}{\cdot}d^{-1}$, on June 3, 2020 with 5.3 $mg{\cdot}m^{-2}{\cdot}d^{-1}$ and on June 23, 2020 with 5.0 $mg{\cdot}m^{-2}{\cdot}d^{-1}$. Northerly winds prevailed during those days and wind speed varied from 2.4 to 3.5 $m{\cdot}s^{-1}$.

At the Lauredal site the highest DSPM levels registered during the restrictions were on May 20, 2020, with 229.7 $mg{\cdot}m^{-2}{\cdot}d^{-1}$ and on June 23, 2020, with 160.8 $mg{\cdot}m^{-2}{\cdot}d^{-1}$. Although on the first of these two days high levels of DSPM were collected at both the Lauredal and EMA sampling sites, the latter corresponds with the date on which minimum DSPM levels were recorded at the EMA site. At the Lauredal site, the three lowest DSPM levels were registered for three samples with similar levels but taken under different meteorological conditions. Two of them were collected on days with winds predominantly from the first and second quadrants (> 80% frequency of counts of wind direction between NW and E in both cases): on April 24, 2020 (37.2 $mg{\cdot}m^{-2}{\cdot}d^{-1}$) and on June 3, 2020 (35.0 $mg{\cdot}m^{-2}{\cdot}d^{-1}$), with mean wind speeds of 2.8 ± 1.6 $m{\cdot}s^{-1}$ and 2.4 ± 1.6 $m{\cdot}s^{-1}$, respectively. The other sample was collected on May 21, 2020 (36.8 $mg{\cdot}m^{-2}{\cdot}d^{-1}$), with similar wind speed (2.7 ± 1.6 $m{\cdot}s^{-1}$) but wind direction predominantly from W and SW (> 65%).

At the Laboratory site, the DSPM levels during restrictions remained below a value of 42.1 $mg{\cdot}m^{-2}{\cdot}d^{-1}$, the maximum DSPM value being recorded on May 22, 2020, with winds from E, NE and W predominantly and wind speeds of 2.5 ± 1.1 $m{\cdot}s^{-1}$ on average. The minimum DSPM levels during this period were registered on May 26, 2020 with 10.4 $mg{\cdot}m^{-2}{\cdot}d^{-1}$ and on May 28, 2020 with 11.7 $mg{\cdot}m^{-2}{\cdot}d^{-1}$, when prevailing winds were from the NE (54% frequency of counts) and mean wind speeds of 3.0 ± 1.1 $m{\cdot}s^{-1}$ and 2.9 ± 15 $m{\cdot}s^{-1}$ respectively.

3.3.3. Dry deposition and maximum gust

Table 5 presents the r_s obtained between DSPM levels registered at each sampling station and their corresponding maximum wind speed. The relationships found between the latter variable and the metals measured in DSPM samples are also included.

A significant negative interdependence ($p < 0.05$) was observed in all the cases, except for K at the Lauredal site. This type of interdependence suggests that there was an inverse relationship between maximum wind speed and the dry deposition levels, which may be explained by the fact that the sampling sites are close to the potential anthropogenic sources of this pollutant. For a particle with certain size and density, and without taking into account other variables like topography, it may be expected that the higher the wind speed, the higher the distance it could

Table 5
Spearman correlation (r_s) coefficient between the levels of DSPM and seven metals and the maximum wind speed at the three sampling stations ('EMA','-Lauredal' and 'Laboratory').

	Maximum wind speed		
	EMA	Lauredal	Laboratory
DSPM	−0.71	−0.37	−0.77
Fe	−0.67	−0.59	−0.75
Ca	−0.71	−0.47	−0.77
Al	−0.69	−0.48	−0.82
Mg	−0.70	−0.48	−0.74
Mn	−0.68	−0.59	−0.75
K	−0.72	0.03*	−0.71
Na	−0.66	−0.41	−0.58

* Indicates non-significant results (p-value ≥ 0.05).

travel from its source. In the regression model developed by Briz-Redón et al. (2022, 2021) to discriminate between the effects of the meteorology and lockdown, a negative association between wind speed and all the pollutants, except for O_3, was found. Furthermore, they highlighted that lower wind speeds may lead to increased levels of deposition (Briz-Redón et al., 2022).

Stronger correlations were found at the EMA ($|r_s| > 0.65$) and Laboratory sites ($|r_s| > 0.70$, except for Na) stations than at the Lauredal site ($|r_s| < 0.6$), which may be explained by the shielding effect caused by the greater presence of buildings in that area.

To sum up, in general significant reductions ($p < 0.05$) were found in the particles and metallic elements in the DSPM fraction during restrictions (except for K at the Lauredal site). However, the highest levels of all the elements were collected under western winds before restrictions, regardless of the sampling site. And during restrictions no sample from this wind direction was collected. Thus, given the variations observed in the wind profile before and during the restrictions, the influence of this variable on the reductions in DSPM levels observed during restrictions cannot be discarded.

4. Conclusions

The results of this study suggest the existence of an important problem of dry deposition in the western area of the Spanish city of Gijón. All the samples collected before COVID-19 restrictions at the industrial suburban station ('EMA') exceeded the Spanish legal limit value for SPM that was in force until 2002 (300 $mg{\cdot}m^{-2}{\cdot}d^{-1}$), reaching values of up to 4898 $mg{\cdot}m^{-2}{\cdot}d^{-1}$. High levels of DSPM were also measured at the two industrial urban stations ('Lauredal' and 'Laboratory'), with maximums of up to 1039.2 $mg{\cdot}m^{-2}{\cdot}d^{-1}$ and 672.7 $mg{\cdot}m^{-2}{\cdot}d^{-1}$, respectively.

Drastic reductions were found in mean DSPM levels when comparing the period of time before the lockdown restrictions and the period during the said restrictions: 97.2, 73.5 and 90.5% at EMA, Lauredal and Laboratory sites, respectively. Regardless of the sampling site, the major constituent of DSPM among the seven elements analysed was Fe, followed by Ca. Important reductions have been found during restrictions in the levels of all these elements, with the exception of K. This element showed lower reductions in its levels at the EMA and Laboratory sites than the other elements and at the Lauredal site its mean value even increased.

As many factors affect atmospheric pollutant levels, the reductions observed in DSPM levels and its constituents might not be caused only by the restriction of population mobility and industrial activity during the lockdown. Indeed, it was found that in general, minimum DSPM levels were collected with winds coming from N-NE and maximums with winds coming from W-SW, regardless of the sampling station. Moreover, a significant negative interdependence was observed between the maximum wind gust and DSPM level at the EMA and the Laboratory sites.

Future air quality policies should consider measures for the reduction of DSPM emissions from anthropogenic sources in order to reduce their impact on industrialized urban/suburban sites.

CRediT authorship contribution statement

Rosa Lara: Investigation, Formal analysis, Writing, Writing – review & editing. **Laura Megido:** Formal analysis, Supervision. **Luis Negral:** Supervision, Methodology, Conceptualization. **Beatriz Suárez-Peña:** Writing – review & editing. **Leonor Castrillón:** Funding acquisition, Project administration, Supervision.

Declaration of competing interest

The authors declare that they have no known competing financial interests or personal relationships that could have appeared to influence the work reported in this paper.

Acknowledgements

This work was supported by the Principality of Asturias Regional Government (project SV-PA-19-06). The authors gratefully acknowledge the contribution of the Principality of Asturias Regional Government and the Gijón City Council in providing the meteorological data, as well as that of the Scientific-Technical Services of the University of Oviedo for providing technical support.

Appendix A. Supplementary data

Supplementary data to this article can be found online at https://doi.org/10.1016/j.atmosenv.2022.119216.

References

Alastuey, A., Querol, X., Aas, W., Lucarelli, F., Pérez, N., Moreno, T., Cavalli, F., Areskoug, H., Balan, V., Catrambone, M., Ceburnis, D., Cerro, J.C., Conil, S., Gevorgyan, L., Hueglin, C., Imre, K., Jaffrezo, J.L., Leeson, S.R., Mihalopoulos, N., Mitosinkova, M., O'Dowd, C.D., Pey, J., Putaud, J.P., Riffault, V., Ripoll, A., Sciare, J., Sellegri, K., Spindler, G., Yttri, K.E., 2016. Geochemistry of PM 10 over Europe during the EMEP intensive measurement periods in summer 2012 and winter 2013. Atmos. Chem. Phys. 16 (10), 6107–6129. https://doi.org/10.5194/acp-16-6107-2016.

Almeida, S.M., Pio, C.A., Freitas, M.C., Reis, M.A., Trancoso, M.A., 2005. Source apportionment of fine and coarse particulate matter in a sub-urban area at the Western European Coast. Atmos. Environ. 39–17, 3127–3138. https://doi.org/10.1016/j.atmosenv.2005.01.048.

Banerjee, T., Murari, V., Kumar, M., Raju, M.P., 2015. Source apportionment of airborne particulates through receptor modeling: Indian scenario. Atmos. Res. 164–165, 167–187. https://doi.org/10.1016/j.atmosres.2015.04.017.

Briz-Redón, Á., Belenguer-Sapiña, C., Serrano-Aroca, Á., 2021. Changes in air pollution during COVID-19 lockdown in Spain: a multi-city study. J. Environ. Sci. 101, 16–26. https://doi.org/10.1016/j.jes.2020.07.029.

Briz-Redón, Á., Belenguer-Sapiña, C., Serrano-Aroca, Á., 2022. A city-level analysis of PM2.5 pollution, climate and COVID-19 early spread in Spain. J. Environ. Heal. Sci. Eng. https://doi.org/10.1007/s40201-022-00786-2.

Carslaw, D.C., Ropkins, K., 2012. Environmental Modelling & Software openair d an R package for air quality data analysis. Environ. Model. Software 27 (28), 52–61. https://doi.org/10.1016/j.envsoft.2011.09.008.

Dall'Osto, M., Booth, M.J., Smith, W., Fisher, R., Harrison, R.M., 2008. A study of the size distributions and the chemical characterization of airborne particles in the vicinity of a large integrated steelworks. Aerosol Sci. Technol. 42 (12), 981–991. https://doi.org/10.1080/02786820802339587.

Figgis, B., Guo, B., Javed, W., Ahzi, S., Rémond, Y., 2018. Dominant environmental parameters for dust deposition and resuspension in desert climates. Aerosol Sci. Technol. 52 (7), 788–798. https://doi.org/10.1080/02786826.2018.1462473.

Gautam, S., Hens, L., 2020. COVID-19: impact by and on the environment, health and economy. Environ. Dev. Sustain. 22, 4953–4954. https://doi.org/10.1007/s10668-020-00818-7.

APG, 2020. Port Authority of Gijón (APG). Annual Report 2019. https://www.puertogijon.es/wp-content/uploads/2020/08/Memoria-2019.pdf. (Accessed 18 June 2021).

Herut, B., Nimmo, M., Medway, A., Chester, R., Krom, M.D., 2001. Dry atmospheric inputs of trace metals at the Mediterranean coast of Israel (SE Mediterranean): sources and fluxes. Atmos. Environ. 35 (4), 803–813.

Hleis, D., Fernández-Olmo, I., Ledoux, F., Kfoury, A., Courcot, L., Desmonts, T., Courcot, D., 2013. Chemical profile identification of fugitive and confined particle

emissions from an integrated iron and steelmaking plant. J. Hazard Mater. 250, 246–255. https://doi.org/10.1016/j.jhazmat.2013.01.080.
Jephcote, C., Hansell, A.L., Adams, K., Gulliver, J., 2021. Changes in air quality during COVID-19 'lockdown'in the United Kingdom. Environ. Pollut. 272, 116011 https://doi.org/10.1016/j.envpol.2020.116011.
Khalifa, S.A.M., Swilam, M.M., El-wahed, A.A.A., Du, M., El-seedi, H.H.R., Kai, G., Masry, S.H.D., Abdel-daim, M.M., Zou, X., Halabi, M.F., 2021. Beyond the pandemic: COVID-19 pandemic changed the face of life. Int. J. Environ. Res. Publ. Health 18 (11), 5645. https://doi.org/10.3390/ijerph18115645.
Kumari, P., Toshniwal, D., 2020. Impact of lockdown on air quality over major cities across the globe during COVID-19 pandemic. Urban Clim. 34, 100719 https://doi.org/10.1016/j.uclim.2020.100719.
Lara, R., Suárez-Peña, B., Megido, L., Negral, L., Rodríguez-Iglesias, J., Fernández-Nava, Y., Castrillón, L., 2021. Health risk assessment of potentially toxic elements in the dry deposition fraction of settleable particulate matter in urban and suburban locations in the city of Gijón, Spain. J. Environ. Chem. Eng. 9 https://doi.org/10.1016/j.jece.2021.106794.
Lovrić, M., Pavlović, K., Vuković, M., Grange, S.K., Haberl, M., Kern, R., 2021. Understanding the true effects of the COVID-19 lockdown on air pollution by means of machine learning. Environ. Pollut. 274, 115900 https://doi.org/10.1016/j.envpol.2020.115900.
Machado, M., Santos, J.M., Reisen, V.A., Reis, N.C., Mavroidis, I., Lima, A.T., 2018. A new methodology to derive settleable particulate matter guidelines to assist policy-makers on reducing public nuisance. Atmos. Environ. 182, 242–251. https://doi.org/10.1016/j.atmosenv.2018.02.032.
Martins, V., Moreno, T., Minguillón, M.C., Van Drooge, B.L., Reche, C., Amato, F., de Miguel, E., Capdevila, M., Centelles, S., Querol, X., 2016. Origin of inorganic and organic components of PM2. 5 in subway stations of Barcelona, Spain. Environ. Pollut. 208, 125–136. https://doi.org/10.1016/j.envpol.2015.07.004.
Mohapatra, K., Biswal, S.K., 2014. Effect of particulate matter (PM) on plants, climate, ecosystem and human health. Int J Adv Technol Eng Sci 2 (4), 2348–7550.
MPRCMD, 2020. Real Decreto 463/2020, de 14 de marzo, por el que se declara el estado de alarma para la gestión de la situación de crisis sanitaria ocasionada por el COVID-19. Ministerio de la Presidencia, Relaciones con las Cortes y Memoria Democrática (MPRCMD). https://www.boe.es/boe/dias/2020/03/14/. (Accessed 15 April 2021).
Nava, S., Lucarelli, F., Amato, F., Becagli, S., Calzolai, G., Chiari, M., Giannoni, M., Traversi, R., Udisti, R., 2015. Biomass burning contributions estimated by synergistic coupling of daily and hourly aerosol composition records. Sci. Total Environ. 511, 11–20. https://doi.org/10.1016/j.scitotenv.2014.11.034.
Negral, L., Suárez-Peña, B., Amado, Á., Megido, L., Lara, R., Marañón, E., Castrillón, L., 2021. Settleable matter in a highly industrialized area: chemistry and health risk assessment. Chemosphere 274, 129751. https://doi.org/10.1016/j.chemosphere.2021.129751.
Pachon, J.E., Weber, R.J., Zhang, X., Mulholland, J.A., Russell, A.G., 2013. Revising the use of potassium (K) in the source apportionment of PM2.5. Atmos. Pollut. Res. 4 (1), 14–21. https://doi.org/10.5094/APR.2013.002.
PRTR, 2020. Spanish Register of Emissions and Pollutant Sources. https://en.prtr-es.es/. (Accessed 21 October 2021).
Querol, X., Alastuey, A., de la Rosa, J., Sánchez-de-la-Campa, A., Plana, F., Ruiz, C.R., 2002. Source apportionment analysis of atmospheric particulates in an industrialised urban site in southwestern Spain. Atmos. Environ. 36 (19), 3113–3125.
Querol, X., Massagué, J., Alastuey, A., Moreno, T., Gangoiti, G., Mantilla, E., Duéguez, J. J., Escudero, M., Monfort, E., Pérez García-Pando, C., Petetin, H., Jorba, O., Vázquez, V., de la Rosa, J., Campos, A., Muñóz, M., Monge, S., Hervás, M., Javato, R., Cornide, M.J., 2021. Lessons from the COVID-19 air pollution decrease in Spain: now what? Sci. Total Environ. 779, 146380 https://doi.org/10.1016/j.scitotenv.2021.146380.
Ravindra, K., Singh, T., Vardhan, S., Shrivastava, A., Singh, S., Kumar, P., Mor, S., 2022. COVID-19 pandemic: what can we learn for better air quality and human health? J. Infect. Public Health 15, 187–198. https://doi.org/10.1016/j.jiph.2021.12.001.
Rodríguez-Urrego, D., Rodríguez-Urrego, L., 2020. Air quality during the COVID-19: PM 2.5 analysis in the 50 most polluted capital cities in the world. Environ. Pollut. 266, 115042 https://doi.org/10.1016/j.envpol.2020.115042.
Salvador, P., Artíñano, B., Alonso, D.G., Querol, X., Alastuey, A., 2004. Identification and characterisation of sources of PM10 in Madrid (Spain) by statistical methods. Atmos. Environ. 38 (3), 435–447.
Shehzad, K., Sarfraz, M., Shah, S.G.M., 2020. The impact of COVID-19 as a necessary evil on air pollution in India during the lockdown. Environ. Pollut. 266, 115080 https://doi.org/10.1016/j.envpol.2020.115080.
Silva, A.C.T., Branco, P.T.B.S., Sousa, S.I.V., 2022. Impact of COVID-19 pandemic on air quality: a systematic review. Int. J. Environ. Res. Publ. Health 19. https://doi.org/10.3390/ijerph19041950.
Tobías, A., Carnerero, C., Reche, C., Massagué, J., Via, M., Minguillón, M.C., Alastuey, A., Querol, X., 2020. Changes in air quality during the lockdown in Barcelona (Spain) one month into the SARS-CoV-2 epidemic. Sci. Total Environ. 726, 138540 https://doi.org/10.1016/j.scitotenv.2020.138540.
Tsai, J.H., Lin, K.H., Chen, C.Y., Ding, J.Y., Choa, C.G., Chiang, H.L., 2007. Chemical constituents in particulate emissions from an integrated iron and steel facility. J. Hazard Mater. 147 (1–2), 111–119. https://doi.org/10.1016/j.jhazmat.2006.12.054.
Watson, J.G., Zhu, T., Chow, J.C., Engelbrecht, J., Fujita, E.M., Wilson, W.E., 2002. Receptor modeling application framework for particle source apportionment. Chemosphere 49 (9), 1093–1136. https://doi.org/10.1016/S0045-6535(02)00243-6.
WHO, 2020. WHO Director-General's opening remarks at the media briefing on COVID-19 - 11 March 2020. https://www.who.int/director-general/speeches/detail/who-director-general-s-opening-remarks-at-the-media-briefing-on-covid-19—11-march-2020. (Accessed 25 July 2021).